Optical channel drop filters based on photonic crystal ring resonators

taalbi ahmed

Optics Communications

Optics Communications 285 (2012) 368–372

Contents lists available at SciVerse ScienceDirect

Optics Communications

journal homepage: www.elsevier.com/locate/optcom

Optical channel drop filters based on photonic crystal ring resonators

Mahmoud Youcef Mahmoud *, Ghaouti Bassou, Ahmed Taalbi, Zoheir Mohamed Chekroun

Department of Physics, Faculty of Science, Djillali Liabes, University of Sidi Bel Abbes, Algeria

A R T I C L E I N F O

Article history:
Received 10 July 2011
Received in revised form 7 September 2011
Accepted 26 September 2011
Available online 11 October 2011

Keywords:
Optical devices
Photonic integrated circuits
Ring resonators
Waveguide
Photonic crystals
FDTD

A B S T R A C T

A new optical channel drop filters (CDFs) configuration based on photonic crystals ring resonators (PCRRs) is provided. The transmission characteristics for single-ring and multiple-ring configurations have been investigated by using the two-dimensional (2D) finite-difference time-domain (FDTD) technique in triangular lattice photonic crystal (PC) silicon rods. Both forward and backward dropping were achieved in dual-ring PCRR structures. In this filter, 100% drop efficiency and acceptable quality factor can be obtained at 1550 nm. The present device can be used in the future photonic integrated circuits.

1. Introduction

Photonic crystals (PCs) are very suitable candidates for realization of future passive and active optical devices because of their ability to control light-wave propagation. Structures based on PCs enable researchers to design small-scale devices. Such structures offer the potential to be integrated into optical circuits. By introducing the defects in the PC structures, various optical components can be realized [1,2].

Channel drop filters (CDFs), on the other hand, are essential components of photonic integrated circuits (PICs) and wavelength division multiplex (WDM) optics communication systems. Various CDFs exist, such as fiber Bragg gratings, Fabry–Perot filters, and arrayed waveguide gratings. Resonant CDFs, which involve waveguide-cavity interaction, are other attractive applicants for this intention [3–5]. Significant progress has been made on CDF based devices in the areas of compactness, high spectral selectivity, wide spectral tunability, fast switching, and low-power switching [6, 7]. Fan et al. [3] reported channel drop filters based on square-lattice 2D PCs. The resonators are consisted of one or two point defects inside the 2D PCs. The size and the refractive index of scatters are varied to match the desired resonance condition. The quality factor of forward and backward drop filters in their results is approximately 1000 and 6000, respectively.

The first report of a photonic-crystal ring resonator (PCRR) was in a hexagonal waveguide ring laser cavity [8], where flexible mode design and efficient coupling were discussed. Later, the spectral characteristics of the waveguide-coupled rectangular ring resonators in photonic crystals were investigated by Kumar et al. [9], where a large single quasi-rectangular ring was introduced as the frequency selective dropping elements. Qiang et al. [10] studied add-drop filters based on square-lattice PCs, thus the resonator comprises a square trace defect in 2D PCs. The quality factor of single square ring filter is enhanced from 160 to over 1000 by increasing the coupling sections between waveguide and ring. They also proposed a dual square ring filter in order to achieve forward dropping. Recently Monifi et al. [11] presented a three output-ports channel drop filter based on the ring structure introduced by Qiang et al. in Ref. [10]. By manipulating the refractive index and radius of some scatters in PCs, they achieved a high transmission, three wavelengths channel drop filter in double-ring configuration. The estimated quality factor based on the reported data is about 100. PCs based ring resonators provide very well optical confinement due to ultra low bending loss. In addition, Bai et al. [12] reported a new 45° PCRR based on square lattice silicon rods. They obtained a quality factor of more than 830 and dropped efficiency of 90% at 1550 nm. It is helpful to overcome the challenge aforementioned by reducing the radius of ring to achieve a resonator with high-Q, high wavelength selectivity, and ultra small footprint size [13].

In this paper, we propose and investigate a new type of optical CDF based on PCRRs. The symmetrical filter consists of a single or dual-PCRRs laterally coupled to a bus waveguide and a drop waveguide using resonant tunnelling process. Its performance is investigated by the 2D FDTD method with the perfectly matched layer (PML) absorbing boundaries conditions at all boundaries. The proposed device provides a possibility of optical channel drop filter and can be used in the future photonic integrated circuits.

* Corresponding author. Tel.: +213 6 62 67 29 63.
E-mail address: mahmoudhamoud@yahoo.com (M. Youcef Mahmoud).

0030-4018/$ – see front matter
doi:10.1016/j.optcom.2011.09.068

2. Single ring photonic crystal ring resonators

All the designs in this paper are based on two-dimensional (2D) triangular lattice of silicon rods (refractive index $n_{Si}=3.46$) in an air background ($n_{air}=1.00$). As shown in Fig. 1(a), the W1 bus waveguide is formed by removing a single line defect (one line of rods removed) along ΓK direction. If the height of the rods is more than two investigated wavelengths, the structure can be considered infinite on the vertical direction, that is, a two-dimensional model instead of practical three dimensional one, which is typically computational time and memory consuming. In addition, it can offer the design trade-offs and guidelines before the real structure design based on a completely 3D FDTD technique [10].

In this investigation, the ratio of the rod radius *r* to the lattice constant *a*, is 0.2. The photonic band gap and the dispersion curve for the guided defect mode in the single line-defect waveguide (W1) were simulated with the free MIT Photonics-Bands (MPB) package [14]. This program computes definite-frequency eigenstates (harmonic modes) of Maxwell's equations in periodic dielectric structures for arbitrary wavevectors, using fully-vectorial and three-dimensional methods. It is especially designed for the study of photonic crystals, but is also applicable to many other problems in optics, such as waveguides and resonator systems. As shown in Fig. 1(b), a photonic band gap (PBG) is found only for the TM polarization. In other words, the proposed structure does not have PBG for transverse electric (TE) modes. Thus, all of simulations are done in TM mode. In addition, there exists a single-mode frequency (normalized) ranging from 0.337 a/λ to 0.442 a/λ below the light line.

For the 1550 nm communication window, the lattice constant *a*, is set at 607.6 nm.

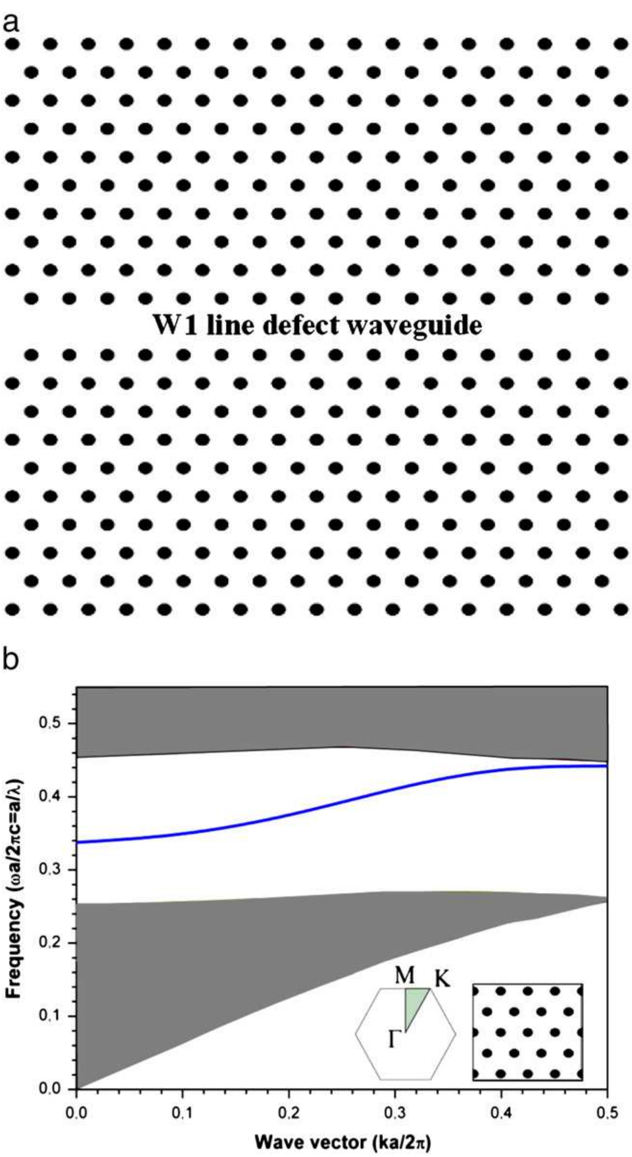

Fig. 1. (a) Single line-defect (W1) photonic crystal waveguide, (b) Dispersion plot for TM polarization and the corresponding guided mode shown as a blue line in the photonic bandgap region.

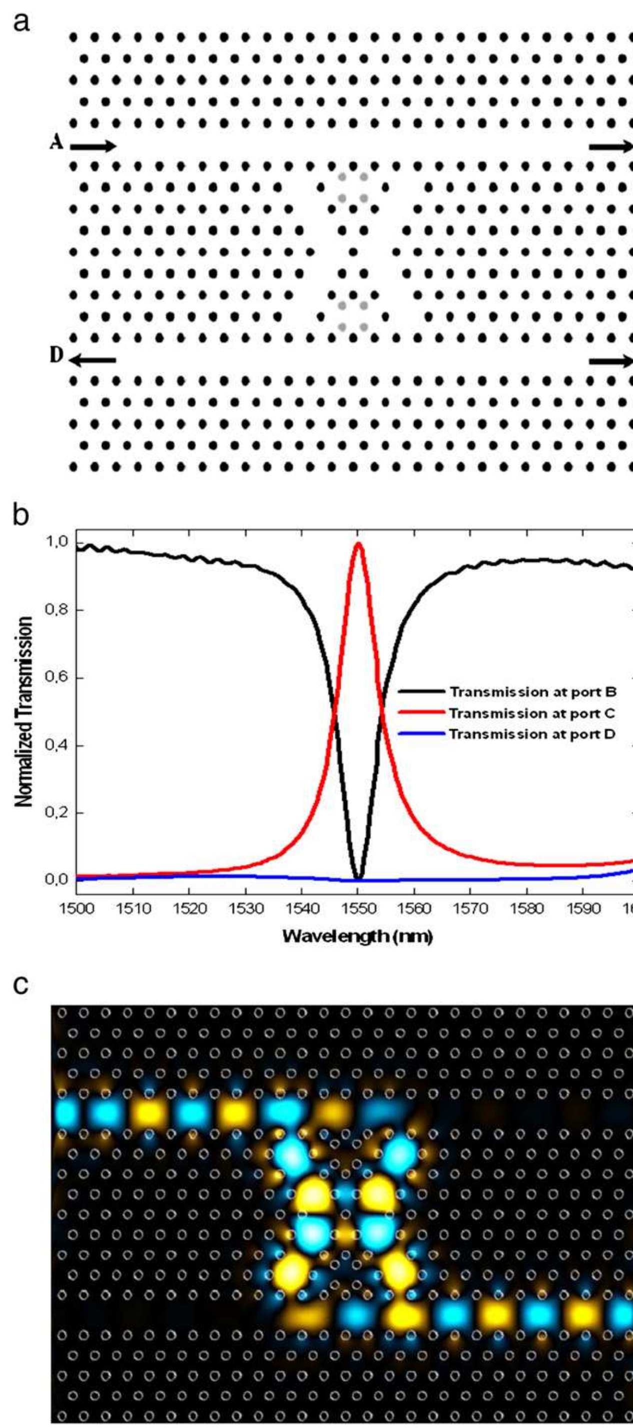

Fig. 2. (a) Schematic of single-ring PCRR based CDFs, (b) Normalized transmission spectra at B, C and D, (c) The electric field pattern at resonant wavelengths of 1550 nm.

The single ring optical CDF is schematically shown in Fig. 2(a), where the incident port and exit ports are labelled as A, B, C, D, respectively. Eight additional extra scattering rods with gray color are introduced to improve the spectral selectivity and obtain a very high dropped efficiency [10]. These scatterers have exactly the same refractive indexes as all other dielectric rods in PC structure and their diameters is chosen to be $r_S = 0.965r$ for better performance.

The transmission characteristics were simulated with the free open two-dimensional finite-difference time-domain (FDTD) technique using perfectly matched layers (PML) as absorbing boundaries [15]. A Gaussian optical pulse, covering the whole frequency-range-of-interest, is launched at the input port A. Power monitors were placed at each of the other three ports (B, C, D) to collect the transmitted spectral power density after Fourier-transformation. All of the transmitted spectral power densities were normalized to the incident light spectral power density from input port A.

The normalized transmission spectra for three output ports (B, C, D) in the single ring CDFs are displayed in Fig. 2(b) as black, red

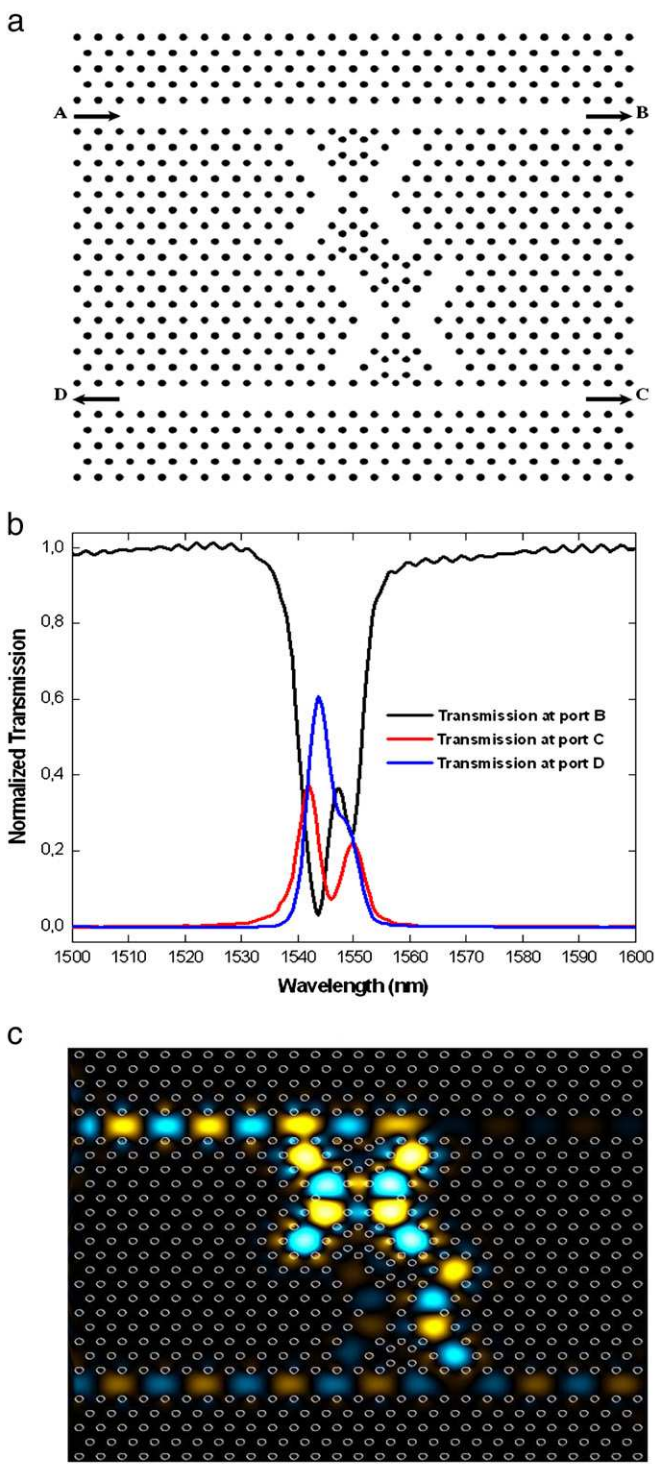

Fig. 3. (a) Schematic of dual-ring PCRR based CDFs for backward dropping, (b) Normalized transmission spectra at B, C and D, (c) The electric field pattern at resonant wavelengths of 1543 nm.

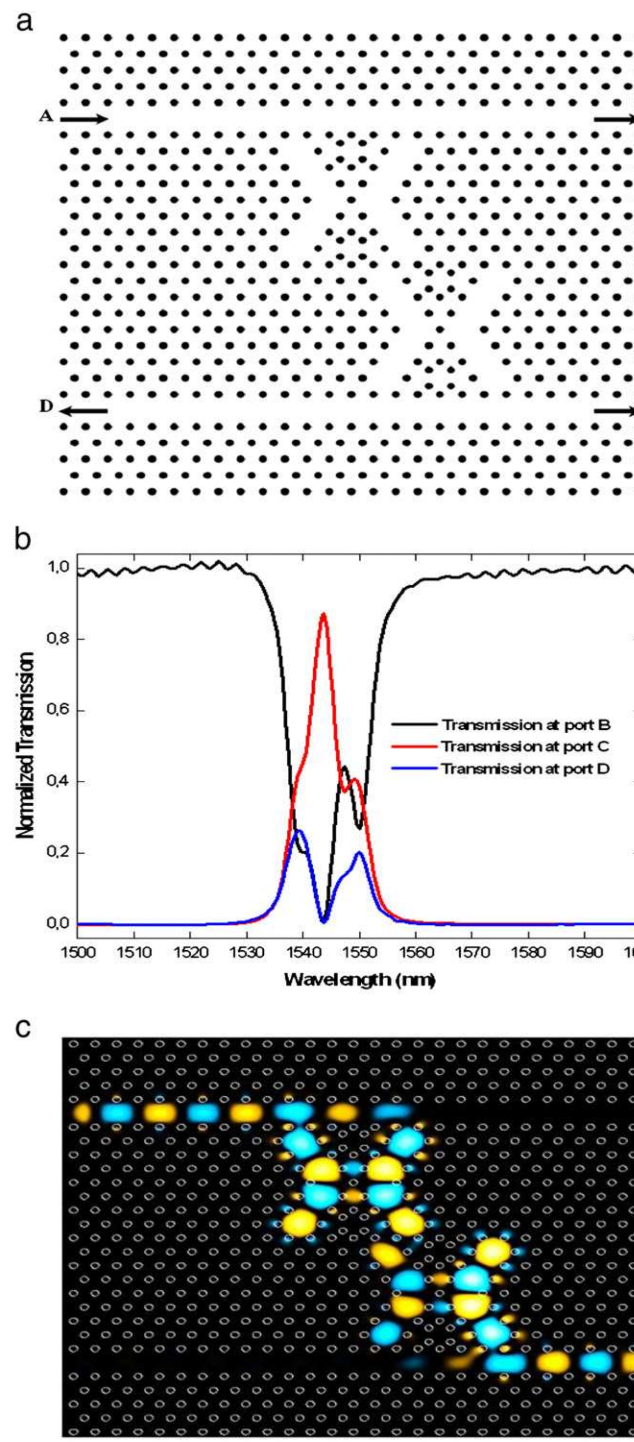

Fig. 4. (a) Schematic of dual-ring PCRR based CDFs for forward dropping, (b) Normalized transmission spectra at B, C and D, (c) The electric field pattern at resonant wavelengths of 1543 nm.

and blue lines, respectively. It can be seen that the spectral selectivity is significantly improved, with close to 100% (>99.98%) drop efficiency; can be achieved at the resonant frequency (1550 nm). In addition, the forward dropping at the port C predominates at λ = 1550 nm, which is obviously different with the dominance of backward dropping at resonance for the traditional resonant single micro-ring structure. The forward dropping is enhanced at certain frequencies, and the particular mechanism is not understood so far [16]. In this case, the incident wave at port A only generates the resonant mode with clockwise traveling, and there is no direct coupling between incident wave and another counter-clockwise traveling mode [17]. However, the clockwise and counterclockwise traveling resonant modes are related by the mutual coupling. So the counter-clockwise resonant mode is improved due to both resonant modes coupling, and then most light-waves are forward dropped at the port C. The quality factor Q of forward dropping peak is 196. Such Q values can be enhanced with further optimization processes. By comparing our new optical CDFs with the related works in above mentioned papers, the spectral selectivity of the proposed one is higher and complete power transfer from the input to the drop port, i.e. forward dropping

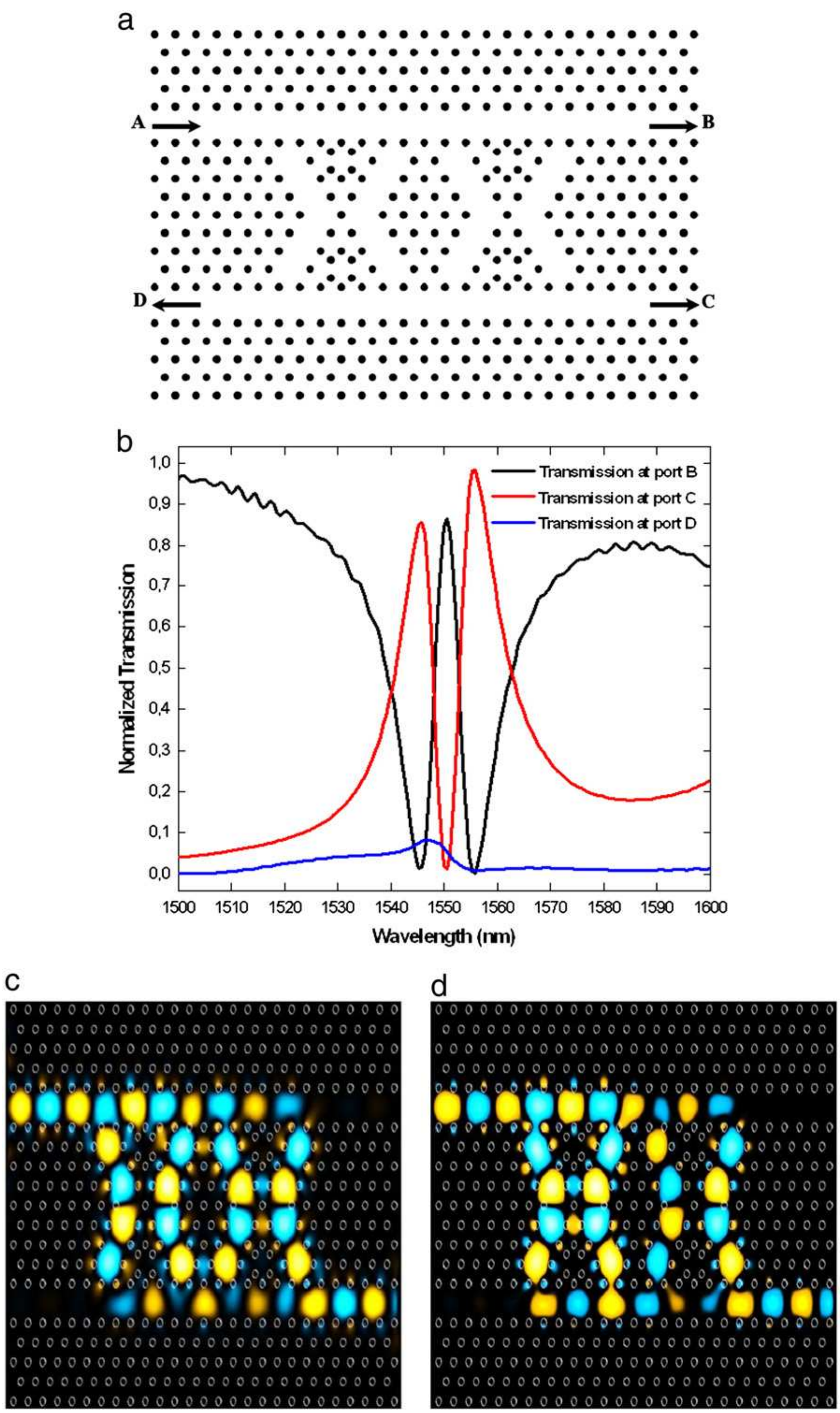

Fig. 5. (a) Schematic of dual-ring PCRR based CDFs for forward dropping in serial configurations, (b) Normalized transmission spectra at B, C and D, (c) The electric field pattern at resonant wavelengths of 1545 nm, (d) The electric field pattern at resonant wavelengths of 1556 nm.

is possible in single-ring PCRRs. Finally, the steady field distribution is obtained by replace the temporal pulsed light source with a mono-wavelength temporally continued light source in FDTD simulation. The wavelength of the light source is set to be the resonant wavelength. The continued light source is launched into input waveguide until the field distribution is stable. Snapshot of channel drop filter (CDF) at resonant wavelengths of 1550 nm is shown in Fig. 2(c).

3. Dual-ring photonic crystal ring resonators

The CDF transfer characteristics in single-ring resonator can be flexibly modified by coupling multiple PCRRs in both parallel and serial configurations. Shown in Fig. 3(a) is the schematic diagram of dual-ring PCRRs, where the distances between two rings along x and y directions are 2*a* and 0*a* respectively. As shown in Fig. 3(b), the normalized transmission spectra at port B, C and D are denoted as black, red and blue lines, respectively. As can be seen, backward dropping efficiency ($\lambda = 1543$ nm) of 60% and Q of 299 can be achieved in parallel configurations. Modes propagate clockwise in both PCRR rings, which results in backward dropping. This clockwise rotation phenomenon has also been observed in dual-ring PCRRs given in Ref. [10]. Snapshot of the electric field distribution at resonant wavelengths of 1543 nm is shown in Fig. 3(c).

The parallel dual-ring PCRRs configuration, where the distance between two rings along x direction increased to 4*a* (*a* is the lattice constant) is shown in Fig. 4(a). Fig. 4(b) describes the transmission spectra at port B, C and D, which are donated by the black, red and blue lines, respectively. Comparing that dropping with the forward dropping characteristics obtained from single-ring PCRRs shown in Fig. 2(b), higher spectral selectivity was obtained with the Q approaching 257 for the dropping channel. However, the dropping efficiency decreased to 87%. In general, there is a trade-off between the increase of the cavity Q and the decrease of the coupling/dropping efficiency [10]. Both backward dropping and forward dropping can be obtained depending upon the coupling strength and the modal symmetry [18,19]. Snapshot of the electric field distribution at resonant wavelengths of 1543 nm is shown in Fig. 4(c).

Shown in Fig. 5(a) is the serial dual-ring PCRRs configuration, where the distances between two rings along x and y directions are 0a and 0a respectively. Fig. 5(b) depicts the normalized transmission spectra in the serial dual-ring configuration, where the power transmission at port B, C and D are denoted by the black, red and blue lines, respectively. It is clear that the dropping channels switched to the other two resonant cavity modes with different symmetry properties at 1545 nm and 1556 nm. This is caused by the mode superposition. At resonance, the resonant field couples to the drop and the input guides. The ring cavity power that couples back into the input guide does so in antiphase with the input signal, resulting in cancellation at the throughput port and making complete power transfer from the input to the drop port possible [10]. The dropped efficiency for the peaks at 1545 nm and 1556 nm are 85% and 96% respectively.

Based on our simulations, the main difference among the three dual-ring structures is the ring coupling, i.e. the number of the shifted dielectric rods between the top and the bottom ring in x direction. The distance between the two rings has been optimized in a separate program and the period of 2*a* and 4*a* leads to obtain acceptable results. In addition, the filter characteristics can be selectively improved and both backward and forward dropping can be realized by controlling the coupling periods in double-ring PCCR structures. High drop efficiency with high quality factor appears feasible, which makes these PCRRs one of the most promising designs for a PC-CDF.

Finally, Fig. 5(c) and Fig. 5(d) show the electric field distribution in the CDF for two forward drop channels at 1545 nm and 1556 nm respectively.

4. Conclusion

In this paper, a new optical channel drop filters based on photonic crystal ring resonators is proposed and numerically demonstrated in two-dimensional triangular lattice silicon rods. Dropped efficiency of 100% can be achieved in single-ring PCRRs at 1550 nm. Both the forward and backward dropping can be achieved by cascading dual-ring PCRRs in parallel and serial configurations. Such structures have the ability to be integrated in the future nanophotonic circuits.

Acknowledgment

The present work was supported by the Ministry of Higher Education and Scientific Research.

References

[1] J.D. Joannopoulos, R.D. Meade, J.N. Winn, Photonic Crystals: Molding the Flow of Light, Princeton University Press, Princeton, NJ, USA, 1995.
[2] H.T. Chien, C.C. Chen, P.G. Luan, Optics Communications 259 (2006) 873.
[3] S. Fan, P.R. Villeneuve, J.D. Joannopoulos, H.A. Haus, Optics Express 3 (1998) 4.
[4] E. Yablonovitch, Physical Review Letters 58 (1987) 2059.
[5] S. John, Journal of Physical Review Letters 58 (1987) 2486.
[6] M. Lipson, IEEE Journal of Lightwave Technology 23 (2005) 4222.
[7] M. Notomi, A. Shinya, S. Mitsugi, E. Kuramochi, H.Y. Ryu, Optics Express 12 (2004) 1551.
[8] S.H. Kim, H.Y. Ryu, H.G. Park, G.H. Kim, Y.S. Choi, Y.H. Lee, Applied Physics Letters 81 (2002) 2499.
[9] V. Dinesh Kumar, T. Srinivas, A. Selvarajan, Photonics and Nanostructures 2 (2004) 199.
[10] Z. Qiang, W. Zhou, R.A. Soref, Optics Express 15 (2007) 1823.
[11] F. Monifi, A. Ghaffari, M. Djavid, M.S. Abrishamian, Applied Optics 48 (2009) 804.
[12] J.B. Bai, J.Q. Wang, X.Y. Chen, J.Z. Jiang, L. Hui, Y.S. Qiu, Z.X. Qiang, Optoelectronics Letters 6 (2010) 0203.
[13] T.T. Maia, F.Li. Hsiaoa, C. Leea, W. Xianga, C.C. Chenc, W.K. Choi, Sensors and Actuators A: Physical 165 (2011) 16.
[14] S.G. Johnson, J.D. Joannopoulos, Optics Express 8 (2001) 173.
[15] A.F. Oskooi, D. Roundy, M. Ibanescu, P. Bermel, J.D. Joannopoulos, S.G. Johnson, Journal of Computer Physics Communications 181 (2010) 687.
[16] H. Ren, J. Zhang, Y. Qin, K. Liu, Z. Wu, W. Hu, C. Jiang, Y. Jin, Optics Communications 284 (2011) 4073.
[17] Z. Zhang, M. Dainese, L. Wosinski, M. Qiu, Optics Express 16 (2008) 4621.
[18] K. Sakoda, Physical Review B: Condensed Matter 52 (1995) 7982.
[19] S.H. Kim, Y.H. Lee, IEEE Journal of Quantum Electronics 39 (2003) 1081.